Amphipathic α-Helix Mediates the Heterodimerization of Soluble Guanylyl Cyclase

Takumi Shiga and Norio Suzuki∗

Division of Biological Sciences, Graduate School of Science, Hokkaido University,

Sapporo 060-0810, Japan

Short title: Heterodimerization of Soluble GC

∗Corresponding author. Tel.: +81-11-706-4908; Fax: +81-11-706-4461.

E-mail address: norio-s@sci.hokudai.ac.jp

ABSTRACT - Soluble guanylyl cyclase (soluble GC) is an enzyme consisting of α and β subunits and catalyzes the conversion of GTP to cGMP. The formation of heterodimer (α_1/β_1 or α_2/β_1) is essential for the catalytic activity. Each subunit has been shown to comprise three functionally different parts: a C-terminal catalytic domain, a central dimerization domain, and an N-terminal regulatory domain. The central dimerization domain in the β_1 subunit, which contains an N-terminal binding site (NBS) and a C-terminal binding site (CBS), have been postulated to be responsible for the formation of α/β heterodimers. In this study, we analyzed heterodimerization by pull down assay using the affinity between histidine tag and Ni^{2+} Sepharose after co-expression of various N- and C-terminally truncated α_1 mutants (FLAG tag) and β_1 wild type (histidine tag) in the baculovirus/Sf9 system, demonstrating that the CBS-like sequence of the α_1 subunit is critical for the formation heterodimer with the β_1 subunit and the NBS-like sequence of the α_1 subunit is essential for the formation of enzymatically active heterodimer, although itself was not involved in heterodimerization. The analysis of the secondary structure of the α1 subunit predicted the existence of an amphipathic α-helix in the residues 431-464. Experiments with site-directed α_1 subunit mutant proteins demonstrated that the amphipathicity of the α-helix is important for the formation of a correct active center in the dimer.

Key words: soluble guanylyl cyclase, cGMP, heterodimer, dimerization domain, recombinant protein, pull down assay, amphipathic α-helix, secondary structure

INTRODUCTION

Both the soluble and membrane forms of guanylyl cyclases (GCs) catalyze the conversion of GTP to cGMP, which is a ubiquitous second messenger in intracellular signaling cascades and responsible for a wide variety of physiological responses (Drewett and Garbers, 1994; Garbers and Lowe, 1994; Garbers *et al*., 1994). Soluble GC is a heterodimer consisting of α and β subunits, and contains a prosthetic ferrous heme group to which nitric oxide (NO) binds with high affinity. Formation of an NO-heme complex and a subsequent conformational change of the heterodimer are responsible for the up to 200-fold increases in the catalytic rate (Gerzer *et al*., 1981; Humbert *et al*., 1990; Stone and Marletta, 1994). In mammals, cDNAs for four soluble GC subunits (α_1, α_2, β_1, and β_2) have been isolated from various tissues (Koesling *et al*., 1988; Koesling *et al*., 1990; Yuen *et al*., 1990; Harteneck *et al*., 1991). Both the α_1/β_1 and α_2/β_1 heterodimers have been shown to be enzymatically active when formed in an *in vitro* expression system (Russwurm *et al*., 1991). A single expression of either one of the subunits has been shown to yield an α_1/α_1- or a β_1/β_1-homodimer, although both homodimers were catalytically inactive (Zabel *et al*., 1999). In previous studies, we have isolated and characterized the cDNA and genomic DNA clones encoding the soluble GC subunits, *OlGCS-*α_1 and *OlGCS-*β_1, both of which are aligned in tandem on the genome of the medaka fish *Oryzias latipes* (Mikami *et al*., 1998, Mikami *et al*., 1999). We recently demonstrated that the medaka fish contains another type of a soluble GC subunit gene, *OlGCS-*α_2, which locates on different linkage group of *OlGCS-*α_1 and *OlGCS-*β_1 (Yao *et al*., 2003).

Each subunit of soluble GC can be divided functionally into three parts: a C-terminal catalytic domain, a central region commonly referred to as the dimerization

domain, and an N-terminal regulatory domain participating in heme-binding (Koesling, 1999). The His^{105} of the β_1 subunit has been identified as the proximal heme ligand site (Wedel *et al*., 1994; Zhao *et al*., 1998; Foerster *et al*., 1996). The C-terminal catalytic domain is highly conserved among various soluble GC subunits and is assigned as being responsible for catalysis based on homology to the related domain of adenylyl cyclase (Koesling, 1999). Dimerization has been attributed to the central region of the soluble GC subunits mainly based on studies with the peptide receptor/membrane GCs (Wilson and Chinkers, 1996). Recently, it has been demonstrated that the dimerization region of the β_1-subunit consists of 205 amino acid residues over the regulatory and central regions and contains a discontinuous site of 41 amino acid residues (N-terminal binding site: NBS) and 30 amino acid residues (C-terminal binding site: CBS), respectively, facilitating binding of the β_1 subunit to the α_1 subunit (Zhou *et al*., 2004). On the other hand, the function of the N-terminal part of the α_1 subunit has been remained to be solved, although there are several papers to demonstrate that the N-terminal part of the α_1 subunit is critical for heme-binding (Wedel *et al*., 1995) and that deletion of the N-terminal 259 amino acids from the α_1 subunit had no effect on the properties of the enzyme at all, and the amino acids 259-364 of the α_1 subunit represent an important functional domain for the transduction of the NO-activation signal (Koglin and Behrends, 2003). Although soluble GC has not been crystallized yet for X-ray diffraction analysis, it has been predicted that its catalytic domain is resemble to that of the class III adenylyl cyclases (Tucker *et al*, 1998; Sunahara *et al*., 1998). Structural analysis of the catalytic core of the adenylyl cyclases demonstrated an antiparallel orientation of the two catalytic domains (C_1 and C_2) with two pockets, each being formed by both the catalytic domains (Zhang *et al*., 1997; Tesmer *et al*., 1997).

To investigate the dimerization region of the α_1 subunit, we generated several recombinant soluble GC subunits in an expression system with Sf9 cells and performed pull down assay using the affinity between histidine tag and Ni^{2+} Sepharose. Here, we report that the CBS-like sequence of OlGCS-α_1 is involved in the formation of heterodimer with OlGCS-β_1 and that the amphipathic α-helix of OlGCS-α_1 is critical for the formation of heterodimer with OlGCS-β_1. We also describe that the NBS-like sequence of OlGCS-α_1 plays an important role in the formation of an enzymatically active heterodimer, although it is not involved in the formation of heterodimer with OlGCS-β_1.

MATERIALS AND METHODS

Construction of plasmid for histidine-tagged OlGCS-β_1-full length protein (FL_{HT})

Total RNA was isolated from the adult brain of *O. latipes* by the acid/guanidinium/thiocyanate/phenol/chloroform extraction method (Chomczynski and Sacchi, 1987). Total RNA (5 μg) was used as the template to synthesize the first strand cDNA using an oligo(dT) primer and Super Script II preamplification system for the first-strand cDNA synthesis (Gibco BRL, Tokyo, Japan) according to the manufacturer's protocol. To obtain a C-terminal histidine-tagged OlGCS-β_1-full length protein (OlGCS-β_1-FL_{HT}), we designed the following primers: 5'-GTG GAT CCA TGT ATG GTT TTG TGA AT-3' and 5'-CGC GTC GAC TTA GTG ATG GTG ATG GTG ATG TGC CTT GTC AGC GTC GCT GC-3'. PCR was performed using *Ex Taq* polymerase (TaKaRa, Otsu, Japan) according to manufacturer's protocol with the following PCR conditions: 30 cycles of 30 sec at 94°C, 30 sec at 50°C, 4 min at 72°C, and a final extension of 5 min at 72°C. The cDNA fragment amplified by the

PCR was purified and subcloned into the plasmid vector pBluescript II KS(-) (Stratagene, La Jolla, California, USA). A *Bam*HI/*Sal*I insert from the *OlGCS-β_1* clone in pBluescript II KS(-) vector was ligated into *Bam*HI/*Sal*I cut pFASTBAC1 vector (Invitrogen Japan K.K., Tokyo, Japan).

Construction of plasmids for FLAG-tagged OlGCS-α_1-full length protein (FL_{FLAG}) and its truncated mutant proteins

To obtain a C-terminal FLAG-tagged OlGCS-α_1-full length protein (OlGCS-α_1-FL_{FLAG}), several N-terminal and C-terminal deletion mutant proteins of OlGCS-α_1, we performed PCR using an *OlGCS-α_1* clone in pBluescript II KS(-) as a template. PCR was performed using *Pfu* polymerase (TaKaRa) according to the manufacturer's protocol with various primers (Table 1). The reaction parameters used for PCR were as follows: 30 cycles of 30 sec at 94^{o}C, 30 sec at each annealing temperature shown in Table 1, and 2 min at 72^{o}C, with a final extension of 5 min at 72^{o}C. Each PCR product was purified and digested by *Spe*I and *Xho*I. Resulting *Spe*I/*Xho*I cut PCR product was subcloned into pFASTBAC1 vector.

Construction of plasmids for C-terminal FLAG-tagged site-directed OlGCS-α_1 mutant proteins

Mutagenesis of *OlGCS-α_1* was performed using the following primers: 5'-GCC CAG GAT GGC AAG AAG AAG CG-3' for L434K, 5'-GGC AGC CAA GGA AAA CGC TCA CC-3' for L445K, 5'-CGC TCA CCA AGC GAA GGA GGA GG-3' for L453K, and 5'-GAT CTT AAG TTT TCC ATT TTC CC-3' for L463K. As a template for the mutagenesis, we used the pFASTBAC1 vector containing C-terminal FLAG-tagged intact *OlGCS-α_1*-full length sequence. The mutagenesis was performed

by the “site-directed and semi-random mutagenesis” procedure (Sawano and Miyawaki, 2000).

Generation of recombinant baculovirus

All clones were checked for correctness of the sequence by DNA sequencing. The sequence was determined by the dideoxy chain termination procedure (Sanger *et al*., 1992) with an ABI PRISM 3100 Genetic Analyzer (Applied Biosystems, Osaka, Japan) and analyzed with GENETYX-MAC/version 7.2.0 software (Software Development, Tokyo, Japan). Recombinant baculovirus of the respective clone was generated according to a BAC-TO-BAC Baculovirus Expression System (Invitrogen Japan K. K.).

Sf9 cell culture, expression of recombinant soluble GC subunit constructs and the mutants, and cytosol preparation

Sf9 cells were cultured in SF-900 II serum-free medium supplemented with 50 μg/ml streptomycin, 50 U/ml penicillin, and 20% fetal bovine serum (FBS). Spinner cultures were grown to a cell density of 3.0 x 10^6 cells/ml and then diluted to 2.0 x 10^6 cells/ml in a tissue culture flask for infection. Ten ml of the culture medium containing Sf9 cells (2.0 x 10^6 cells/ml) were infected by each virus stock of OlGCS-α_1 or co-infected with OlGCS-β_1-FL_{HT}-containing virus (ratio 1:1), and continued to culture for 4 days at 37^{o}C. All subsequent experiments were carried out at 4^{o}C. Cells were harvested by centrifugation at 1,000 g for 5 min. The resulting pellet was washed in 1 ml of ice-cold phosphate-buffered saline (PBS), pH 6.2, and then resuspended in 500 μl of an ice-cold lysis buffer for pull down assay (50 mM phosphate buffer, pH 7.2 containing 100 mM NaCl, 10% glycerol, and 0.1% protease inhibitor mixture in DMSO solution) (Wako, Osaka, Japan) or a lysis buffer for assay of GC activity (20 mM

Tris-HCl, pH 6.8, 90 mM NaCl, 10 % glycerol, and 0.1% protease inhibitor mixture-dimethylsulfoxide (DMSO) solution). The suspension was sonicated and then centrifuged at 15,000 g for 20 min, and the resulting supernatant fraction was collected and used for further experiments.

Determination of protein concentration, Western blotting, and pull down assay

Protein concentration was determined by the BCA method using BCA protein assay reagent (PIERCE, Rockford, Illinois, USA). Before each pull down assay, the similar expression level of the protein in each lysate was confirmed by sodium dodecyl sulfate-polyacrylamide gel electrophoresis (SDS-PAGE) and Western blotting. The cell lysate was subjected to SDS-PAGE on a 10% polyacrylamide gel and transferred to a PVDF membrane. The membrane was blocked with 2% dry milk in TPBS (PBS, pH 7.4, containing 0.1% Tween 20) for 15 min at room temperature, rinsed, and incubated overnight at 4^{o}C with anti-His-Tag antibody (MBL, Nagoya, Japan) or ANTI-FLAG M2 monoclonal antibody-alkaline phosphatase conjugate (SIGMA, Saint Louis, Missouri, USA) in TPBS containing 0.2% dry milk. Subsequently, the anti-His-Tag antibody-treated membrane was incubated with secondary antibody for 1 h at room temperature. Immunoreacted proteins were detected using the CDP-Star, ready-to-use (Roche, Tokyo, Japan) or Western blotting detection reagents (Amersham). The density of each band was determined by scanned image using Scion Image Beta 4.0.2 (Scion corporation, Frederick, Maryland, USA). The lysis buffer for pull down assay containing 500 μg protein was incubated overnight at 4^{o}C with 150 μl of chelating Sepharose (Amersham Pharmacia Biotech, Tokyo, Japan), which was preincubated in a total volume of 600 μl containing 75 μl of 0.2 M $NiCl_2$ for 5 min according to the manufacture's protocol. The sample was washed 3 times with 750 μl of the ice-cold

lysis buffer for pull down assay, and then washed 3 times with 300 μl of the ice-cold lysis buffer for pull down assay containing 15 mM imidazole. Proteins were eluted with the ice-cold lysis buffer for pull down assay containing 150 mM imidazole. Eluted proteins were subjected to SDS-PAGE and Western blotting as described above.

Assay of GC activity

Before the assay of GC activity, the similar expression level of the protein in each cytosolic fraction was confirmed by SDS-PAGE and Western blotting. GC activity of the cytosolic fraction (50 μg protein/assay tube) was determined in a total volume of 250 μl by incubation for 15 min at 37^{o}C in an assay solution (50 mM Tris-HCl, pH 7.5, 4 mM $MgCl_2$, 0.5 mM 3-isobutyl-1-methylxanthine (IBMX), 7.5 mM creatine phosphate, 25 U/ml creatine phosphokinase, and 1 mM GTP) with or without 1 mM sodium nitroprusside dihydrate (SNP). The reaction was stopped by boiling for 3 min, and then each assay tube was centifugated at 15,000 g for 10 min. cGMP in the supernatant was determined by cGMP enzyme immunoassay system (Amersham Biosciences, Tokyo, Japan).

RESULTS AND DISCUSSION

Identification of N-terminal binding site (NBS) and C-terminal binding site (CBS) of OlGCS-α_1

To assign the putative NBS- and CBS-like sequences of OlGCS-α_1, the amino acid sequence of OlGCS-α_1 was aligned with that of rat soluble GC-α_1. Sequence identities of the NBS-like sequence of OlGCS-α_1 at positions 280-321 and the CBS-like

sequence of OlGCS-α_1 at position 448-477 to that of the corresponding rat soluble GC-α_1 were 45.2 and 90%, respectively. To define the binding ability of the NBS-like sequence of OlGCS-α_1 or the CBS-like sequence of OlGCS-α_1 to OlGCS-β_1, we generated FLAG-tagged N-terminal deletion mutants or C-terminal deletion mutants of OlGCS-α_1 (Fig. 1), and either one was expressed or co-expressed with the OlGCS-β_1-FL_{HT} in Sf9 cells.

To examine the binding ability of the NBS-like sequence to OlGCS-β_1-FL_{HT}, we performed pull down assay (Fig. 2A). OlGCS-α_1-FL_{FLAG}, OlGCS-α_1[280-678]$_{FLAG}$ or OlGCS-α_1[322-678]$_{FLAG}$ did not bind to Ni^{2+} Sepharose when each construct was expressed without *OlGCS-β_1-FL_{HT}*. Both OlGCS-α_1[280-678]$_{FLAG}$ and OlGCS-α_1[322-678]$_{FLAG}$ fully retained their ability to bind to OlGCS-β_1-FL_{HT}, judging from the result that each OlGCS-α_1 N-terminal deletion protein was detected in the Ni^{2+} Sepharose-binding fraction. This suggests that the NBS-like sequence of OlGCS-α_1 (280-321) is not involved in the heterodimerization with OlGCS-β_1.

We then examined the binding ability of the C-terminal deletion mutant proteins of OlGCS-α_1 to OlGCS-β_1. Co-expression of *OlGCS-α_1[1-448]$_{FLAG}$* or *OlGCS-α_1[1-477]$_{FLAG}$* with *OlGCS-β_1-FL_{HT}* was followed by pull down assay and Western blotting. As shown in Fig. 2B, OlGCS-α_1[1-448]$_{FLAG}$ did not exhibit the binding ability to OlGCS-β_1-FL_{HT}, and no protein band was detected in the Ni^{2+} Sepharose-binding fraction of α_1[1-448]$_{FLAG}$/β_1-FL_{HT} by anti-FLAG antibody. Conversely, OlGCS-α_1[1-477]$_{FLAG}$ bound to OlGCS-β_1-FL_{HT}, suggesting that the CBS-like sequence of OlGCS-α_1 contains the structural elements mediating heterodimerization with OlGCS-β_1-FL_{HT}.

To examine the GC activity of the N-terminal deletion mutant proteins of OlGCS-α_1, *OlGCS-α_1-FL_{FLAG}*, *OlGCS-α_1[280-678]$_{FLAG}$* or *OlGCS-α_1[322-678]$_{FLAG}$* was

co-expressed with *OlGCS-β_1-FL_{HT}* in Sf9 cells and the GC activity of the each cytosolic fraction was measured. As shown in Fig. 3, $\alpha_1[280\text{-}678]_{FLAG}/\beta_1\text{-}FL_{HT}$ showed the basal and SNP-stimulated GC activity at almost the same extent as that of the control soluble GC ($\alpha_1\text{-}FL_{FLAG}/\beta_1\text{-}FL_{HT}$), although $\alpha_1\text{-}[322\text{-}678]_{FLAG}/\beta_1\text{-}FL_{HT}$ did not exhibit GC activity with and without SNP. Therefore, we presume that the NBS-like sequence of OlGCS-α_1 (amino acids 280-321) plays an important role to form the correct active center with the counterpart. This is in good agreement with the results that the β_1 subunit lacking amino acids at position 204-303 (containing NBS: amino acids positions 204-244) failed to show the GC activity when co-expressed with the α_1 subunit, although it exhibits the binding ability to the α_1 subunit at a reduced level (Zhou *et al*., 2004). In a recent study, it was reported that an N-terminal binding site of bovine α_1 subunit (amino acids position 61-128) plays major important role in heterodimerization (Wagner *et al*., 2005). However, in this study, we did not observed such ability in the amino acids position 61-128. In the present study with the pull down assay and the assay of GC activity, we obtained the results to show that OlGCS-$\alpha_1[280\text{-}678]_{FLAG}$ could form heterodimer with OlGCS-β_1-FL_{HT}.

Identification of amphipathic α-helix mediating heterodimerization between OlGCS-α_1 and OlGCS-β_1

To obtain further understanding on the nature of the CBS-like sequence of OlGCS-α_1 for heterodimerization and GC activity, we carried out prediction of the secondary structure of OlGCS-α_1 by the PredictProtein server (http://www.embl-heidelberg.de/predictprotein/) and found that OlGCS-α_1[431-464] is able to form an amphipathic α-helix structure (Fig. 4). It has been reported that amphipathic α-helix often mediates protein-protein interactions (Carr *et al*, 1991).

Therefore, we examined whether the amphipathic α-helix in the α_1-subunit could mediate heterodimerization of both subunits of soluble GC after introduction of site-directed mutation to the α_1-subunit. To disturb the amphipathicity of the α-helix, we focused the four Leu residues (Leu^{434}, Leu^{445}, Leu^{452}, and Leu^{463}) as shown in dotted boxes in Fig. 4B, all of which were predicted to be located intensively on the one side of the α-helix. Various site-directed mutant proteins were generated as described in Materials and Methods. According to the prediction of the secondary structure of the α_1 subunit by the PredictProtein server, the α-helix structure should be maintained even after these four Leu residues were converted to Lys residues leading to loss of amphipathicity. *OlGCS-α_1-L434K$_{FLAG}$*, *L445K$_{FLAG}$*, *L463K$_{FLAG}$*, *L434,445,463K$_{FLAG}$*, or *L434,445,452,463K$_{FLAG}$* was co-expressed with *OlGCS-β_1-FL$_{HT}$* in Sf9 cells and the GC activity of the each cytosolic fraction was measured with or without SNP. As shown in Fig. 5, α_1-L434K$_{FLAG}$/β_1-FL$_{HT}$ or α_1-L445K$_{FLAG}$/β_1-FL$_{HT}$ showed the basal and SNP-stimulated GC activities at almost the same extent as those of α_1-FL$_{FLAG}$/β_1-FL$_{HT}$, but α_1- L463K$_{FLAG}$/β_1-FL$_{HT}$, L434,445,463K$_{FLAG}$/β_1-FL$_{HT}$ or L434,445,452,463K$_{FLAG}$/β_1-FL$_{HT}$ did not show the basal GC activity nor the SNP-stimulatable GC activity. To investigate the binding ability of each site-directed mutant protein to OlGCS-β_1-FL$_{HT}$, we performed pull down assay. As shown in Fig. 6, the binding ability of OlGCS-α_1-L434,445,463K$_{FLAG}$ or OlGCS-α_1-L434,445,452,463K$_{FLAG}$ to OlGCS-β_1-FL$_{HT}$ was remarkably reduced, although α_1-L434K$_{FLAG}$ or α_1-L445K$_{FLAG}$ maintained its binding ability to OlGCS-β_1-FL$_{HT}$. These results suggest that the amphipathicity in the putative α-helix region of OlGCS-α_1 is important to form heterodimer with OlGCS-β_1.

The amphipathicity of the α-helix in OlGCS-α_1[1-448]$_{FLAG}$ would be incomplete because of lacking the C-terminal half of the putative amphipathic α-helix (see Fig 1).

Therefore, we presume that it is one of the major reasons why OlGCS-α_1[1-448]$_{FLAG}$ did not exhibit the binding ability to OlGCS-β_1. Surprisingly, OlGCS-α_1-L463K$_{FLAG}$ also maintained its binding ability to OlGCS-β_1-FL$_{HT}$, although the α_1-L463K$_{FLAG}$/β_1-FL$_{HT}$ did not exhibit any GC activity, suggesting that the formation of heterodimer of OlGCS-α_1 with OlGCS-β_1 is not sufficient for exhibiting the GC activity, probably due to inadequate heterodimerization which leads to formation of inadequate active center. As shown in Fig. 4A, Leu^{463} is conserved among soluble GC-α_1 subunits of various species and located in the C-terminal end of the amphipathic α-helix. For enzymatically active heterodimer formation, it seems to be essential that the correct active center between the catalytic domains of α and β subunit is formed. Conversion of Leu^{463} to Lys in OlGCS-α_1 might lead the detachment of the hydrophobic bond in the C-terminal end of the amphipathic α-helix, although the rest of the amphipathic α-helix maintains the hydrophobic bonds. The detachment of this region appears to lead to the incorrect active center formation between the both subunit catalytic domains. This might be the case that L463K$_{FLAG}$/β_1-FL$_{HT}$ did not show any GC activity.

As shown in Fig. 4A, the amino acid sequence in this region varies among soluble GC α_1 subunits of various species and the changes in the amino acid sequence did not affect the formation of the putative amphipathic α-helix, suggesting that the amphipathic α-helix plays a critical role in the heterodimerization of soluble GC α_1 subunit with soluble GC β_1 subunit. In addition, the analysis of the secondary structure of OlGCS-β_1 by the PredictProtein server predicted that OlGCS-β_1[367-395] forms an amphipathic α-helix, and similar analysis of OlGCS-α_2 also resulted in prediction that OlGCS-α_2[535-555] forms an amphipathic α-helix. These strongly suggest that the amphipathic α-helix mediates the heterodimerization of soluble GC α_1 subunit with soluble GC β_1 subunits.

ACKNOWLEGEMENTS

We are grateful to the staff members of the Center for Advanced Science and Technology, Hokkaido University, for the use of their laboratory facilities. This study was supported by a Grant-in-Aid for Scientific Research from the Ministry of Education, Science, Sports, and Culture of Japan (no. 11236202) and by the National Project on Protein Structural and Functional Analyses.

REFERENCES

Carr DW, Stofko-hahn RE, Fraser ID, Bishop SM, Acott TS, Brennan RG, Scott JD (1991) Interaction of the regulatory subunit (RII) of cAMP-dependent protein kinase with RII-anchoring proteins occurs through an amphipathic helix binding motif. J Biol Chem 266: 14188-14192

Chomczynski P, Sacchi N (1987) Single-step method of RNA isolation by acid guanidinium thiocyanate-phenol-chloroform extraction. Anal Biochem 162: 156-159

Drewett JG, Garbers DL (1994) The family of guanylyl cyclase receptors and their ligands. Endocr Rev 15: 135-162

Foerster J, Harteneck C, Malkewitz J, Schultz G, Koesling D (1996) A functional heme-binding site of soluble guanylyl cyclase requires intact N-termini of α_1 and β_1 subunits. Eur J Biochem 240: 380-386

Garbers DL, Koesling D, Schultz G (1994) Guanylyl cyclase receptors. Mol Biol Cell 5: 1-5

Garbers DL, Lowe DG (1994) Guanylyl cyclase receptors. J Biol Chem 269: 30741-30744

Gerzer R, Böhme E, Hofmann F, Schultz G (1981) Soluble guanylate cyclase purified from bovine lung contains heme and copper. FEBS Lett 132: 71-74

Harteneck C, Wedel B, Koesling D, Malkewitz J, Böhme E, Schultz G (1991) Molecular cloning and expression of a new alpha-subunit of soluble guanylyl cyclase. Interchangeability of the alpha-subunits of the enzyme. FEBS Lett 292: 217-222

Humbert P, Niroomand F, Fischer G, Mayer B, Koesling D, Hinsch KD, Gausepohl H,

Frank R, Schultz G, Böhme E (1990) Purification of soluble guanylyl cyclase from bovine lung by a new immunoaffinity chromatographic method. Eur J Biochem 190: 273-278

Koesling D (1999) Studying the structure and regulation of soluble guanylyl cyclase. Methods 19: 485-493

Koesling D, Herz J, Gausepohl H, Niroomand F, Hinsch KD, Mulsch A, Böhme E, Schultz G, Frank R (1988) The primary structure of the 70 kDa subunit of bovine soluble guanylate cyclase. FEBS Lett 239: 29-34

Koglin M, Behrends S (2003) A functional domain of the α1 subunit of soluble guanylyl cyclase is necessary for activation of the enzyme by nitric oxide and YC-1 but is not involved in heme binding. J Biol Chem 278: 12590-12597

Mikami T, Kusakabe T, Suzuki N (1998) Molecular cloning of cDNAs and expression of mRNAs encoding alpha and beta subunits of soluble guanylyl cyclase from medaka fish *Oryzias latipes*. Eur J Biochem 253: 42-48

Mikami T, Kusakabe T, Suzuki N (1999) Tandem organization of medaka fish soluble guanylyl cyclase α_1 and β_1 subunit genes. Implications for coordinated transcription of two subunit genes. J Biol Chem 274: 18567-18573

Russwurm M, Behrends S, Harteneck C, Koesling D (1998) Functional properties of a naturally occurring isoform of soluble guanylyl cyclase. Biochem J 335: 125-130

Sanger F, Nicklen S, Coulson AR (1992) DNA sequencing with chain-terminating inhibitors. 1977. Biotechnology 24: 104-108

Sawano A, Miyawaki A (2000) Directed evolution of green fluorescent protein by a new versatile PCR strategy for site-directed and semi-random mutagenesis. Nucleic Acids Res 28: E78.

Stone JR, Marletta MA (1994) Soluble guanylate cyclase from bovine lung: activation

with nitric oxide and carbon monoxide and spectral characterization of the ferrous and ferric state. Biochemistry 33: 5636-5640

Sunahara RK, Beuve A, Tesmer JJ, Sprang SR, Garbers DL, Gilman AG (1998) Exchange of substrate and inhibitor specificities between adenylyl and guanylyl cyclase. J Biol Chem 273: 16332-16338

Tesmer JJ, Sunahara RK, Gilman AG, Sprang SR (1997) Crystal structure of the catalytic domains of adenylyl cyclase in a complex with Gsα GTPγS. Science 278: 1907-1916

Tucker CL, Hurley JH, Miller TR, Hurley JB (1998) Two amino acid substitutions convert a guanylyl cyclase, Ret GC-1, into an adenylyl cyclase. Proc Natl Acad Sci USA 95: 5993-5997

Wagner C, Russwurm M, Jäger R, Friebe A, Koesling D (2005) Dimerizaion of NO-sensitive guanylyl cyclase requires the α_1 N terminus. J Biol Chem 280:17687-17693

Wedel B, Harteneck C, Foerster J, Friebe A, Schultz G, Koesling D (1995) Functional domains of soluble guanylyl cyclase. J Biol Chem 270: 24871-24875

Wedel B, Humbert P, Harteneck C, Foerster J, Malkewitz J, Böhme E, Schultz G, Koesling D (1994) Mutation of His-105 in the β_1 subunit yields a nitric oxide-insensitive form of soluble guanylyl cyclase. Proc Natl Acad Sci USA 91: 2592-2596

Wilson EM, Chinkers M (1995) Identification of sequences mediating guanylyl cyclase dimerization. Biochemistry 34: 4696-4701

Yao Y, Yamamoto T, Tsutsumi M, Matsuda M, Hori H, Naruse K, Mitani H, Shima A, Asakawa S, Shimizu N, Suzuki N (2003) Genomic structure and expression of the soluble guanylyl cyclase α_2 subunit gene in the medaka fish *Oryzias latipes*. Zool

Sci 20: 1293-1304

Yuen PS, Potter LR, Garbers DL (1990) A new form of guanylyl cyclase is preferentially expressed in rat kidney. Biochemistry 29: 10872-10878

Zabel U, Hausler C, Weeger M, Schmidt HH (1999) Homodimerization of soluble guanylyl cyclase subunits. Dimerization analysis using a glutathione s-transferase affinity tag. J Biol Chem 274: 18149-18152

Zhang G, Liu Y, Ruoho AE, Hurley JH (1997) Structure of the adenylyl cyclase catalytic core. Nature 386: 247-253

Zhao Y, Schelvis JP, Babcock GT, Marletta MA (1998) Identification of histidine 105 in the β_1 subunit of soluble guanylate cyclase as the heme proximal ligand. Biochemistry 37: 4502-4509

Zhou Z, Gross S, Roussos C, Meurer S, Müller-Esterl W, Papapetropoulos A (2004) Structural and functional characterization of the dimerization region of soluble guanylyl cyclase J Biol Chem 279: 24935-24943

Legends to Figures

Fig. 1. Schematic representation of various OlGCS-α_1 constructs.
The NBS-like sequence (280-321) is represented by the hatched boxes and the CBS-like sequence is defined by dotted boxes. Numbers denote the relative positions of amino acids. A bold line indicates the predicted amphipathic α-helix region.

Fig.2. Pull down assay on the NBS-like or the CBS-like sequence.
Sf9 cells were infected by baculovirus containing an *OlGCS-α_1-FL_{FLAG}*, its N-terminal deletion mutants (A) or its C-terminal deletion mutants (B) with or without *OlGCS-β_1-FL_{HT}*. Almost equal amount of OlGCS-β_1-FL_{HT} was detected in the Ni^{2+} Sepharose-binding fraction by Western blotting (WB) using anti-HT antibody (top). The Ni^{2+} Sepharose-binding fraction was analyzed by Western blotting with anti-FLAG antibody (upper middle). To confirm the protein expression levels in the lysate, Western blotting was performed using anti-HT antibody or anti-FLAG antibody (lower middle and bottom, respectively). Similar results were obtained in two independent experiments.

Fig. 3. The GC activity of N-terminal deletion mutant proteins.
The GC activity in the lysate prepared from respective infected Sf9 cells was assayed with (black columns) or without (white columns) SNP. The activity represent means $\pm$ S.E.M. obtained from three independent experiments.

Fig. 4. The sequence and helical wheel diagram of the amphipathic α-helix of OlGCS-α_1.

(A) The amino acid sequences of the putative amphipathic α-helix of various soluble GC α_1 subunits were aligned. Identical residues are marked by asterisks and the hydrophobic residues were shaded. Numbers denote the relative positions of the amino acids. (B) Hydrophobic amino acid residues are boxed and the Leu residues modified by site-directed mutagenesis are covered with dotted boxes.

Fig. 5. The GC activity of site-directed mutant proteins.

The GC activity in the lysate prepared from respective infected Sf9 cells was assayed with (black columns) or without (white columns) SNP. The activity represents means ± S.E.M. obtained from three independent experiments.

Fig. 6. Pull down assay of site-directed mutant proteins.

Sf9 cells were infected by baculovirus containing *OlGCS-α_1-FL_{FLAG}* or its site-directed mutants with *OlGCS-β_1-FL_{HT}*. The fractions containing the Ni^{2+} Sepharose-binding activity were analyzed by Western blotting with anti-FLAG antibody. The density of each band of the Ni^{2+} Sepharose-binding proteins reacted with anti-FLAG antibody was estimated using Scion image. The data are expressed by fold density relative to the α_1-FL_{FLAG}/β_1-FL_{HT} as 1 and represent means ± S.E.M. obtained from three independent experiments. *$P < 0.05$ for the comparison with α_1-$L434K_{FLAG}$/β_1-FL_{HT} or α_1-$L445K_{FLAG}$/β_1-FL_{HT}.

Table1　Primers and the annealing temperature used for construction of plasmids for OlGCS-α_1-FL_{FLAG} and its truncated mutants

	Sequence of primers	Annealing temperature
a1-FLFLAG		44°C
a1start-SpeI	5'-ACTAGTATGTTCTGCGGCCAAGTTGAA-3'	
a1endFLAG*XhoI	5'-CTCGAGTCACTTGTCATCGTCGTCCTTGTAGTCTTTTTTTGTAAGTTTTGACA-3'	
a1[280-678]FLAG		44°C
a1-dN279	5'-ACTAGTATGACCTCTGCTGGAACGCTCCC-3'	
a1endFLAG*XhoI	5'-CTCGAGTCACTTGTCATCGTCGTCCTTGTAGTCTTTTTTTGTAAGTTTTGACA-3'	
a1[322-678]FLAG		
a1-dN321	5'-ACTAGTATGGGACTTAGAAGGTCTCCCAC-3'	44°C
a1endFLAG*XhoI	5'-CTCGAGTCACTTGTCATCGTCGTCCTTGTAGTCTTTTTTTGTAAGTTTTGACA-3'	
a1[1-477]		
a1start-SpeI	5'-ACTAGTATGTTCTGCGGCCAAGTTGAA-3'	54°C
a1-dC477	5'-CTCGAGTCACTTGTCATCGTCGTCCTTGTAGTCCTGCCACAGCTGCTGGGCCA-3'	
a1[1-448]		54°C
a1start-SpeI	5'-ACTAGTATGTTCTGCGGCCAAGTTGAA-3'	
a1-dC448	5'-CTCGAGTCACTTGTCATCGTCGTCCTTGTAGTCGTTTTCCAAGGCTGCCTTGG-3'	

Fig. 1

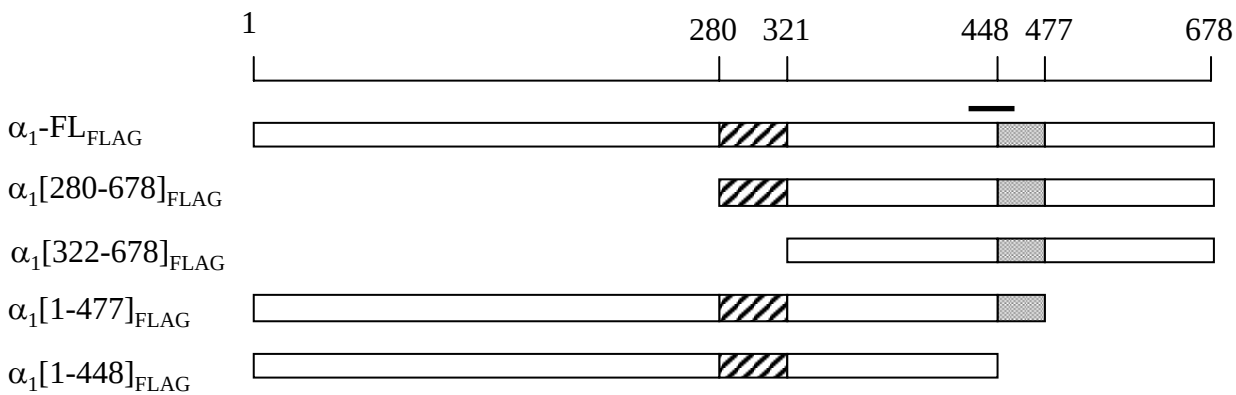
1
280
321
448
477
678
α1-FLFLAG
α1[280-678]FLAG
α1[322-678]FLAG
α1[1-477]FLAG
α1[1-448]FLAG

Fig. 2

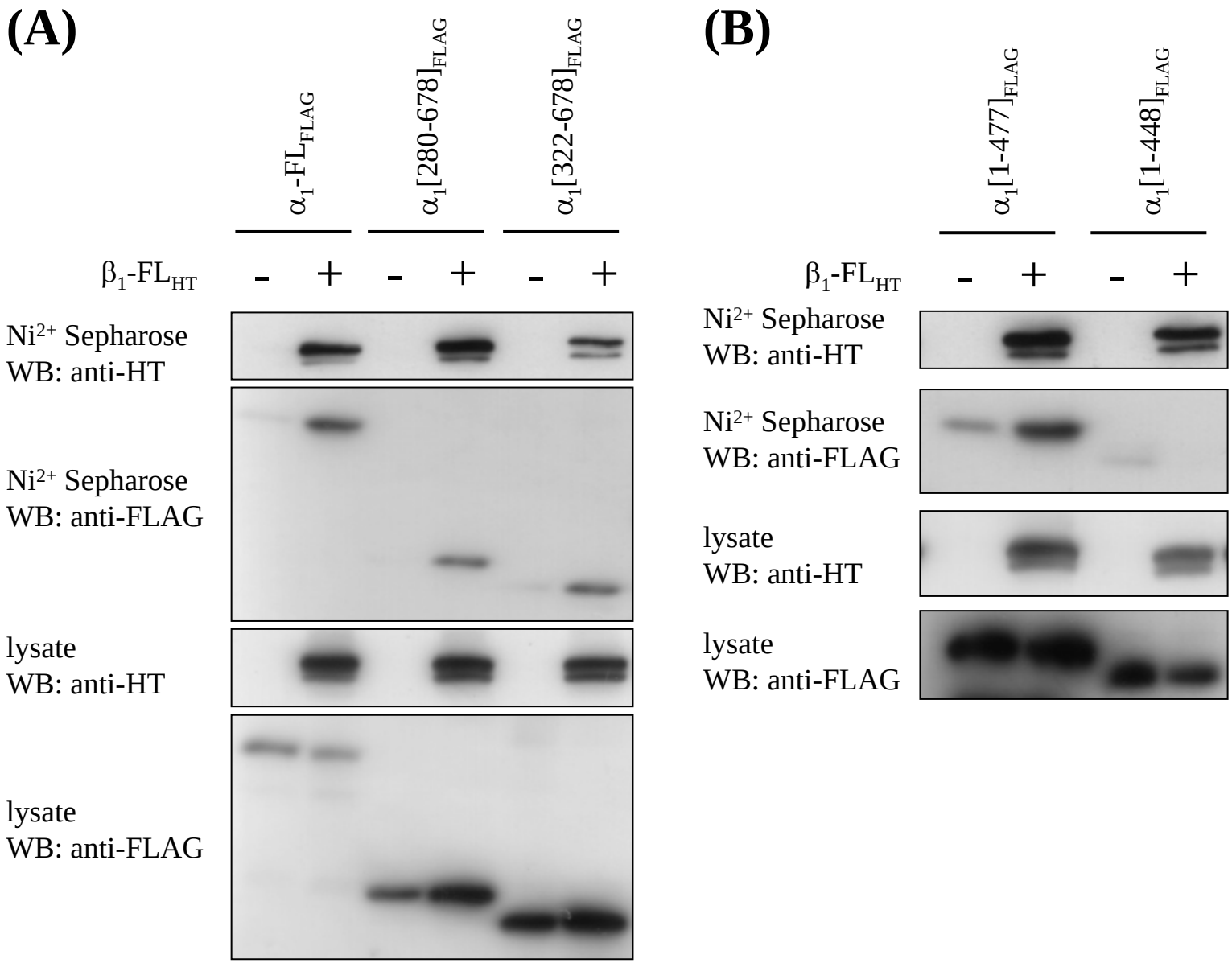
(A)
α1-FLFLAG
α1[280-678]FLAG
α1[322-678]FLAG
β1-FLHT
- + - + - +
Ni2+ Sepharose
WB: anti-HT
Ni2+ Sepharose
WB: anti-FLAG
lysate
WB: anti-HT
lysate
WB: anti-FLAG
(B)
α1[1-477]FLAG
α1[1-448]FLAG
β1-FLHT
- + - +
Ni2+ Sepharose
WB: anti-HT
Ni2+ Sepharose
WB: anti-FLAG
lysate
WB: anti-HT
lysate
WB: anti-FLAG

Fig. 3

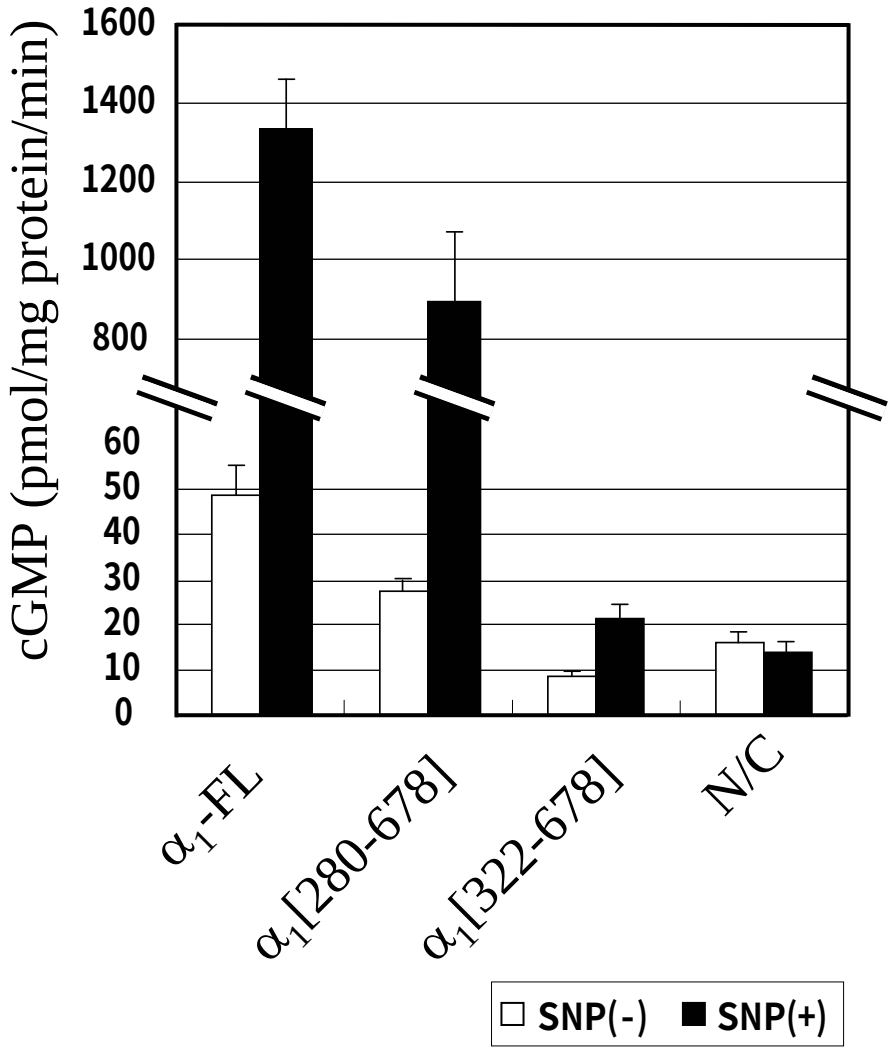
cGMP (pmol/mg protein/min)
1600
1400
1200
1000
800
60
50
40
30
20
10
0
α1-FL
α1[280-678]
α1[322-678]
N/C
SNP(-)
SNP(+)

Fig. 4

(A)

```
mouse       421 QDGLKKRLGKLKATLEHAHQALEEEKKRTVDLLC 455
rat         420 QDGLKKRLGKLKATLEHAHQALEEEKKKTVDLLC 454
human       421 QDGLKKRLGKLKATLEQAHQALEEEKKKTVDLLC 455
medaka      431 QDGLKKRLGKAKAALENAHQALEEEKKKTVDLLF 464
Drosophila  406 QDGLRRRMDKIKNSIEEANSAVTKERKKNVSLLH 440
Manduca     422 QDGLRRRMDKLKNSIEEASKAVDKEREKNVSLLH 456
                ****  *  * *  * *  *   *    * **
```

(B)

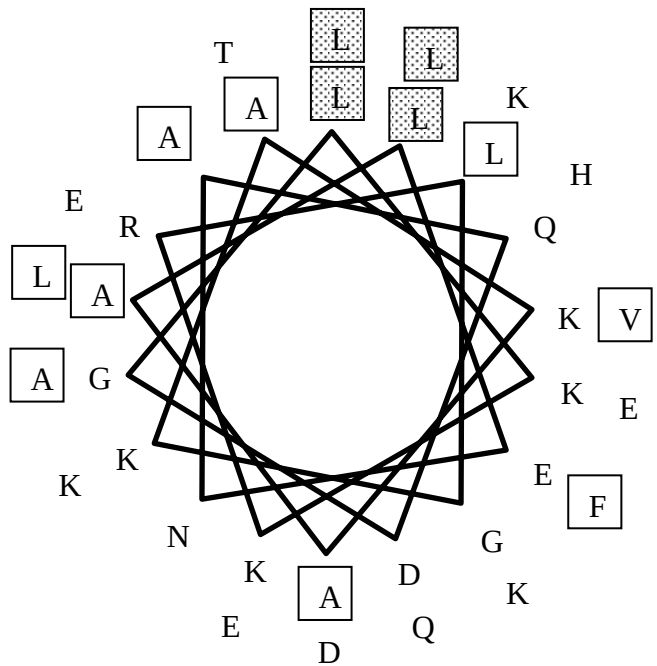

Fig. 5

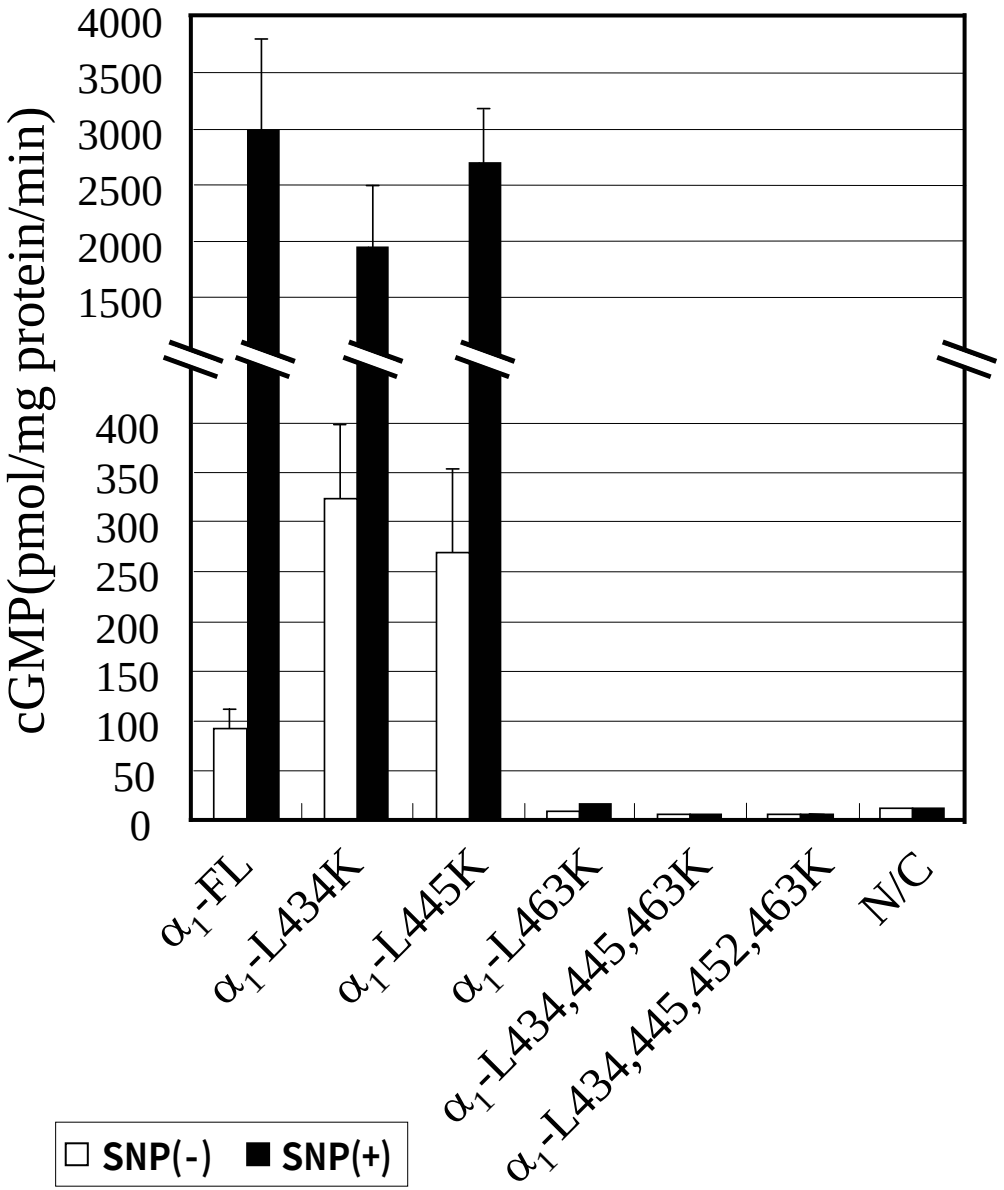
cGMP(pmol/mg protein/min)
4000
3500
3000
2500
2000
1500
400
350
300
250
200
150
100
50
0
α1-FL
α1-L434K
α1-L445K
α1-L463K
α1-L434,445,463K
α1-L434,445,452,463K
N/C
SNP(-)
SNP(+)

Fig. 6

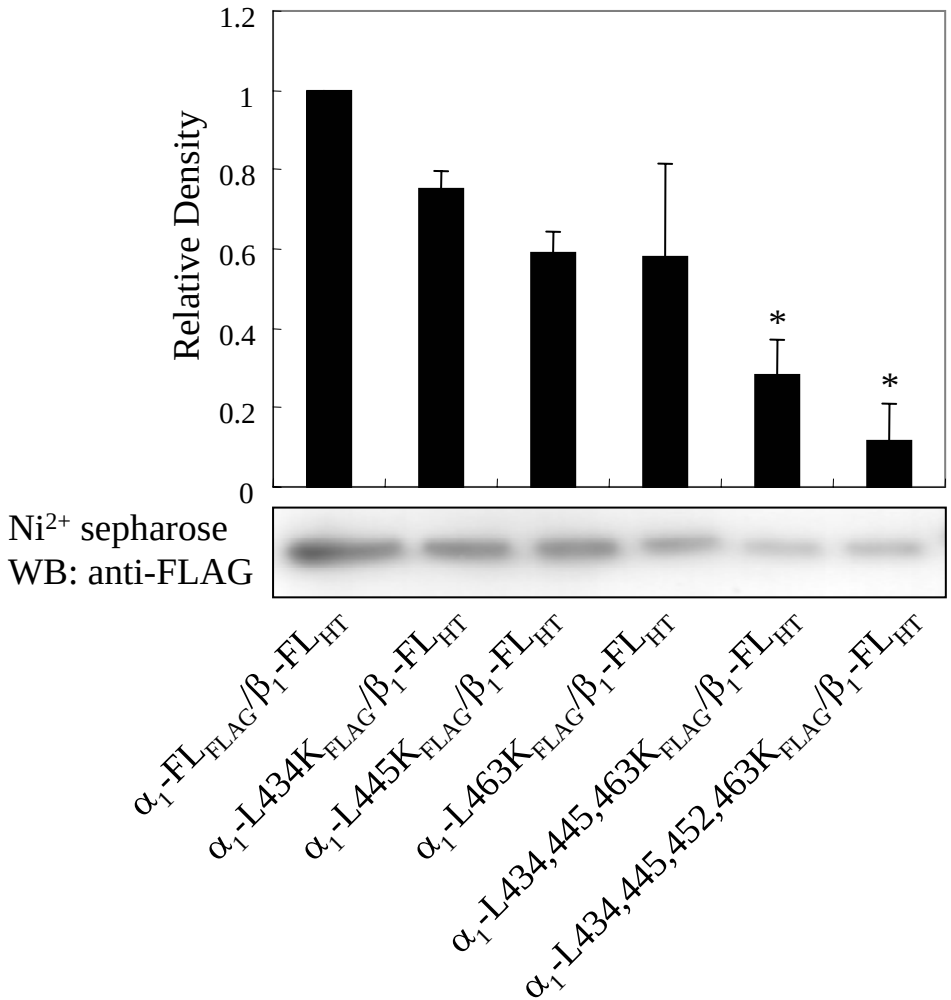
1.2
1
0.8
0.6
0.4
0.2
0
Relative Density
*
*
Ni2+ sepharose
WB: anti-FLAG
α1-FLFLAG/β1-FLHT
α1-L434KFLAG/β1-FLHT
α1-L445KFLAG/β1-FLHT
α1-L463KFLAG/β1-FLHT
α1-L434,445,463KFLAG/β1-FLHT
α1-L434,445,452,463KFLAG/β1-FLHT